Locally modified charge-density waves in Na intercalated VSe_2 studied by scanning tunneling microscopy and spectroscopy

Inger Ekvall,* Hans E. Brauer, Erik Wahlström, and Håkan Olin
Physics and Engineering Physics, Chalmers University of Technology, SE-412 96 Göteborg, Sweden
(Received 13 October 1998)

We have observed local effects of the charge-density wave (CDW) in *in situ* Na-intercalated $1T$-VSe_2 using scanning tunneling microscopy and spectroscopy between 300 and 60 K. Na intercalates nonuniformly, and divides the sample into intercalated (*I*) and nonintercalated (NI) areas. Below the CDW transition temperature these areas displayed totally different CDW's. The NI areas seemed unaffected by Na, and showed a 4×4 CDW that did not differ from the CDW in pure VSe_2. The intercalated areas showed a strong octahedral CDW ($\lambda_1=0.99$ nm, $\lambda_2=0.68$ nm, $\angle 70°$, rotated 20° with respect to the atomic lattice) occurring in three different orientations. Additional spots in Fourier space at low temperatures were interpreted to originate from Na ordering in a 1.3×1.3 $R45°$ structure. Spectroscopy showed a shift of the V $3d$-derived state below the Fermi level (E_F) upon intercalation. In the NI areas, a shift toward E_F (-60 meV compared to -80 meV in pure VSe_2) was observed, while the *I* areas showed a shift away from E_F (-150 meV). The CDW energy gap was enlarged in the *I* areas ($\Delta\approx230$ meV compared to $\Delta\approx80$ meV in pure VSe_2), while it was never resolved in the NI areas. [S0163-1829(99)06511-X]

I. INTRODUCTION

The layered transition metal dichalcogenides (TMD's) consist of one transition-metal atom in between two chalcogen atoms forming covalently bonded sheets with formula MX_2, where M is a transition metal and X are chalcogen atoms. Adjacent sheets are bonded to each other with weak van der Waals forces, leading to highly anisotropic properties. The anisotropy of the materials leads to interesting properties connected to the quasi-low-dimensionality, and TMD's therefore serve as model systems for two-dimensional phenomena. Among the interesting properties are the formation of charge-density waves (CDW's) that occurs in many, but not all, TMD's, and the possibility of intentional modification by intercalation of foreign atoms and molecules in between the layers. A CDW is a standing wave of electron density that does not necessarily coincide with the atomic lattice. Usually, different incommensurate (IC) and commensurate (*C*) phases exist in different temperature ranges. The CDW state is caused by electron-phonon interaction, and therefore, does compete with the superconducting state, to which it has many similarities. As in a superconducting state, a CDW state is characterized by a transition temperature (T_C), an energy gap (2Δ), and particle pairing. The electron-phonon interaction induces a condensate of electron-hole pairs, leading to a standing electron-density wave with a wavelength of $2k_F$, and a density of states depletion (energy gap) at the Fermi level (E_F). Theoretically, a strictly one-dimensional material would be insulating below the transition temperature, while in reality most materials become semimetallic. The CDW phenomenon was predicted in the 1950s, and has been widely studied since then.

When evaporated onto TMD's in ultrahigh vacuum, alkali metals can form intercalation compounds of form R_xMX_2, where R is an alkali metal.[1,2] Upon intercalation, there is a transfer of valence charge from the alkali metal to the host lattice, that changes the electronic properties of the host material. Particularly, a CDW state is likely to be influenced by alkali intercalation, but the expected effects may depend strongly on the detailed changes in the Fermi-surface topology.

We have studied Na intercalation in the layered TMD $1T$-VSe_2 by variable temperature scanning tunneling microscopy (STM) and spectroscopy (STS). Pure VSe_2 has been studied with various techniques by a number of different authors, including Eagelsham, Withers, and Bird[3] van Landuyt, Wiegers, and Amelinckx,[4] and Tsutsumi.[5] The observed CDW structures differ greatly, but presently there is a general agreement of a transition at 110 K. The in-plane 4×4 initial phase has been claimed to be both IC (Ref. 6) and *C* (Ref. 5), and changes of the CDW phase at ~80 K have been observed, both for the in-plane and the interplane components,[5,7,8] that could originate from an IC-*C* transition. STM studies of VSe_2 at 4.2 and 77 K have been published by Coleman and co-workers[9,10] and by Kim, Park, and Olin,[11] showing the 4×4 CDW and an energy gap $\Delta\approx40$ meV at 4.2 K.[10] The electronic band structure of VSe_2 has been extensively studied at room temperature by a variety of techniques,[12–17] and has also been calculated theoretically.[17–19]

Intercalation of Na in VSe_2 has been investigated by different techniques, where the band structure along with magnetic and electronic properties of the intercalated material has been studied,[17,20,21] but low-temperature measurements on Na_xVSe_2 are rare. Magnetic measurements were published by Wiegers and co-workers,[20,22,23] where anomalies in the conductivity and magnetic susceptibility were ascribed to a CDW. In addition, diffuse scattering in electron diffraction of $Na_{0.5}VSe_2$ is believed to originate from CDW's but this has not been further investigated.

In a previous photoemission (PES) and STM study of Na-intercalated VSe_2 at room temperature, we have shown

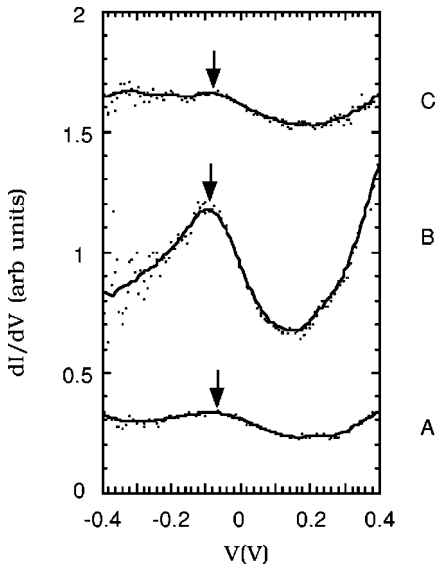

FIG. 1. Room-temperature spectra showing the V $3d$ peak below E_F. (*A*) Pure VSe_2 ~ -85 meV. (*B*) Intercalated areas of Na_xVSe_2 ~ -90 meV. (*C*) Nonintercalated areas of Na_xVSe_2 ~ -80 meV. Solid lines are curve fits to the 256 discrete STS points.

that the intercalated Na atoms are nonuniformly distributed below the first layer, leading to intercalated (*I*) and nonintercalated (NI) areas.[24] In the intercalated areas, small holelike features are found due to locally missing Na. A preliminary low-temperature STS study indicates that the intercalated Na influence the CDW, but the details have not been made clear.[25]

In the present work we focus on the influence of Na intercalation in VSe_2 at low temperatures (60–110 K). Na induced a nonhexagonal CDW at the *I* areas, while the NI areas still showed the presence of a 4×4 CDW that seemed to be unaffected by the intercalation. The band structure was changed by a shift of the strong V $3d$-derived state just below E_F, and by an increase of the CDW energy gap in the *I* areas. These types of studies are useful for understanding the formation and modification of CDW's.

II. EXPERIMENTAL DETAILS

The experiments were made in a UHV STM with variable-temperature facilities (Omicron Vakuumphysik GmbH). The samples were cleaved in air and transferred to the microscope via a fast-entry load-lock chamber. Most of the samples, but not all, were heated to $\sim 300\,^{\circ}C$ to remove contamination. The W tips were electrochemically dc etched, and cleaned inside the UHV by sputtering and heating.[26] Na was evaporated from a home-built breakseal ampoule source, calibrated to evaporate ~ 1 ML in 15 min. The base pressure in the system was 6×10^{-11} mbar and the pressure did not increase during evaporation. Measurements were made from 300 to 60 K, where cooling was made by a He flow cryostat that was temperature controlled by counter-resistive heating. Tunneling spectra were measured with a tunneling resistance of the order of GΩ. The spectra were taken in a grid across the surface, and spectra from similar surface structures were then averaged. The polarity of the applied bias voltage, V_t, corresponds to sample bias. Atomic resolution images were corrected for distortion by using the known hexagonal unit cell of VSe_2, that has a lattice parameter of 0.335 nm.

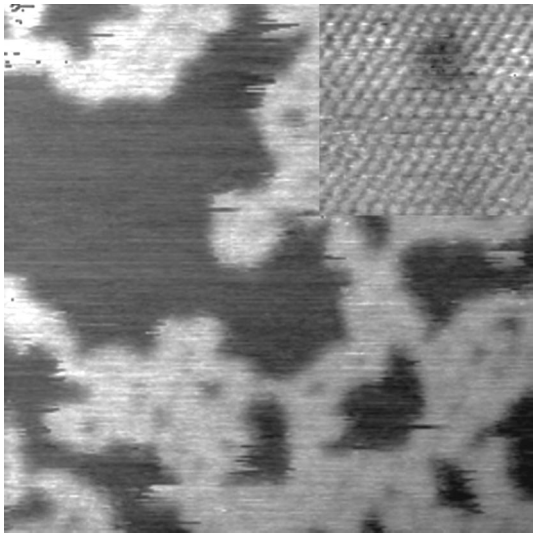

FIG. 2. Na_xVSe_2 at room temperature exhibiting nonintercalated (dark) and intercalated (bright) areas. In the intercalated areas, holes of locally missing Na are seen. Scan size $100\times100\,nm^2$, $V_t=-109$ mV and $I_t=1.79$ nA. Inset: Atomic resolution image of an intercalated area. Inside the ''holes,'' atoms are still visible, excluding the possibility of the holes being lattice defects. Scan size $4\times4\,nm^2$, $V_t=-107$ mV, and $I_t=0.646$ nA.

III. RESULTS

A. Room temperature

The clean VSe_2 surface had large atomically flat areas, with a trigonal atomic arrangement. The atomically resolved images were distorted due to electronic drift in the microscope, but the lattice constant was close to the expected 0.335 nm. No room-temperature images of the pure material are shown here, since they agree with our earlier results.[24] From experiments and theoretical band calculations, a strong mainly V $3d$-derived state is known to exist at ~ 100 meV below E_F.[12,13,17–19] In our STS data, Fig. 1 (curve *A*), it was detected as a peak in dI/dV at ~ 85 meV below E_F.

Evaporation of $\leqslant 1$ ML Na at room temperature showed the expected nonuniform distribution with dark and bright areas of size 20–100 nm, as seen in Fig. 2. The bright areas correspond to areas with Na below the first layer, forming ''two-dimensional islands,'' that causes the material to expand locally to accommodate the Na atoms in the van der Waals gap between the layers. A step height of 1.6 Å between the areas was found together with ''holes'' of locally missing Na below the first layer in the intercalated Na islands, in agreement with our earlier study.[24] Effects of Na below the second layer and further down are presumed to be negligible since STM is a surface-sensitive technique. STS at the *I* areas, Fig. 1 (curve *B*), showed the V $3d$ peak at ~ 90 meV below E_F, while at the NI areas, Fig. 1 (curve *C*), it was found at ~ -80 meV.

B. Low temperature

1. Pure VSe_2

When lowering the temperature, VSe_2 undergoes a transition to a 4×4 CDW state at ~ 110 K. In our STM images of

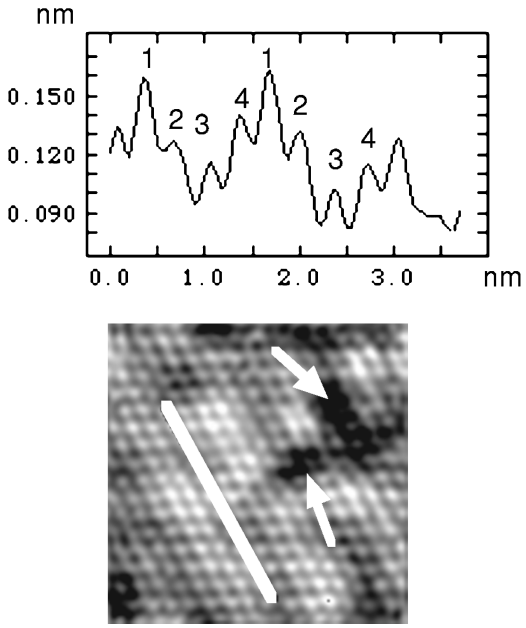

FIG. 3. STM image of the 4×4 CDW in pure VSe_2. In the cross section it can be seen that every fourth atom is enhanced. The white bar shows the position of the cross section. Scan size 5×5 nm^2, $V_t=34$ mV, $I_t=1.715$ nA, and $T=60$ K. Note the lattice defects (marked by arrows).

the pure samples, we clearly saw this 4×4 CDW below 110 K, shown in Fig. 3. The corrugation was about 0.1 Å, i.e., of the same order as the atomic corrugation. Figure 4 (curve *A*) shows low-temperature tunneling spectroscopy of the pure material, where the V $3d$ peak at ~-80 meV and also a CDW energy gap $\Delta\approx80$ meV are seen. This energy gap was not resolved in every measurement, but was proved to be

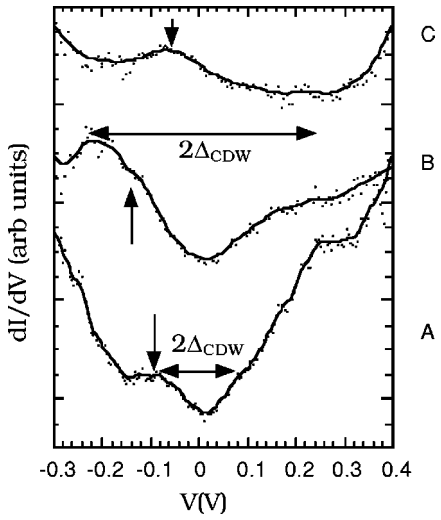

FIG. 4. Spectra taken at 60 K. Arrows mark the position of the V $3d$ state. The energy gap edges are chosen in the middle of the flat range above E_F in the tunneling spectra, before the conductance is increased further. (*A*) Pure VSe_2, with an energy gap of $\Delta\approx80$ meV and the V $3d$ peak at ~-80 meV. (*B*) Intercalated areas of Na_xVSe_2, with $\Delta\approx230$ meV and the V $3d$ peak at ~-150 meV. (*C*) Nonintercalated areas of Na_xVSe_2, with no energy gap and the V $3d$ peak at ~-60 meV. Solid lines are curve fits to the 256 discrete STS points.

very tip dependent. Tip changes while scanning could suddenly cause the gap to appear or disappear, while the V $3d$ peak was still resolved. However, we tried different tips and samples and, when resolved, we repeatedly found the same energy gap. We found no significant gap changes with temperature below T_C.

2. Intercalated Na_xVSe_2

When lowering the temperature in the intercalated samples, we saw two totally different CDW's in the two different areas, as seen in Fig. 5. The NI parts showed a weak 4×4 CDW, similar to the CDW in pure VSe_2. This CDW was not distorted by the presence of Na in the islands nearby. In the *I* islands, we found a strong superstructure that greatly differed from the 4×4 CDW in the NI areas. When analyzing the superstructure in Fourier space, we found that it consisted of a distorted hexagonal pattern, i.e., an octahedral pattern, rotated with respect to the atomic lattice. After distortion correction using the known lattice constant (0.335 nm for pure VSe_2), the wavelength of this distorted pattern was 0.93 ± 0.04 nm in one direction and 0.65 ± 0.04 nm in the two other directions, and the rotation of the long component was $(30\pm4)°$ with respect to the atomic lattice. In Na_xVSe_2 the lattice parameter has been measured by neutron diffraction to 0.348 or 0.373 nm depending on the coordination of the intercalated atoms,[21] which would give us a slightly longer wavelength of the superstructure. We consistently use the pure VSe_2 lattice parameter, since we do not know the effect of the nonuniform distribution on the lattice constant. The relationship between the atomic lattice and the superstructure, that represents the main characteristics of the CDW wavelength, would, however, not differ if we used another lattice constant. Figure 6 shows the resulting structure in real space, that also can be considered as an octahedral superstructure with $\lambda_1=0.99$ nm and $\lambda_2=0.68$ nm, $\angle70°$, where the λ_1 component is rotated 20° counterclockwise with respect to the atomic lattice. This superstructure was incommensurate down to temperatures of 60 K, and occurred in three different orientations, rotated 120° with respect to each other. Different orientations were sometimes found in the same Na island (Fig. 7). These domains did not show sharp boundaries, but changed gradually over a distance of a few nanometers.

Looking further into the fast Fourier transform (FFT), Fig. 8, we found extra spots corresponding to a square period with a wavelength of 0.44 nm, i.e., just slightly longer than the lattice parameter. The two directions of the square symmetry were rotated $+15°$ and $-15°$, respectively, with respect to two of the three host lattice symmetry directions. These FFT spots were only found at the *I* parts at low temperatures, and as they followed the rotation of the Na-induced CDW, we interpreted these as an effect of Na ordering at low temperatures.

When scanning at a very low bias, the corrugation of the CDW in the NI areas was enhanced, from ~0.1 Å at 100 mV to ~0.5 Å at 2 mV, regardless of polarity. The corrugation of the CDW in the *I* areas was of the order of 0.5 Å at 100 mV, and was also enhanced at low bias to ~1–3 Å. Cross-section lines showing the corrugation for different scanning parameters are found in Fig. 9. In the STM images we could clearly see the enhancement of the pure CDW, since it could

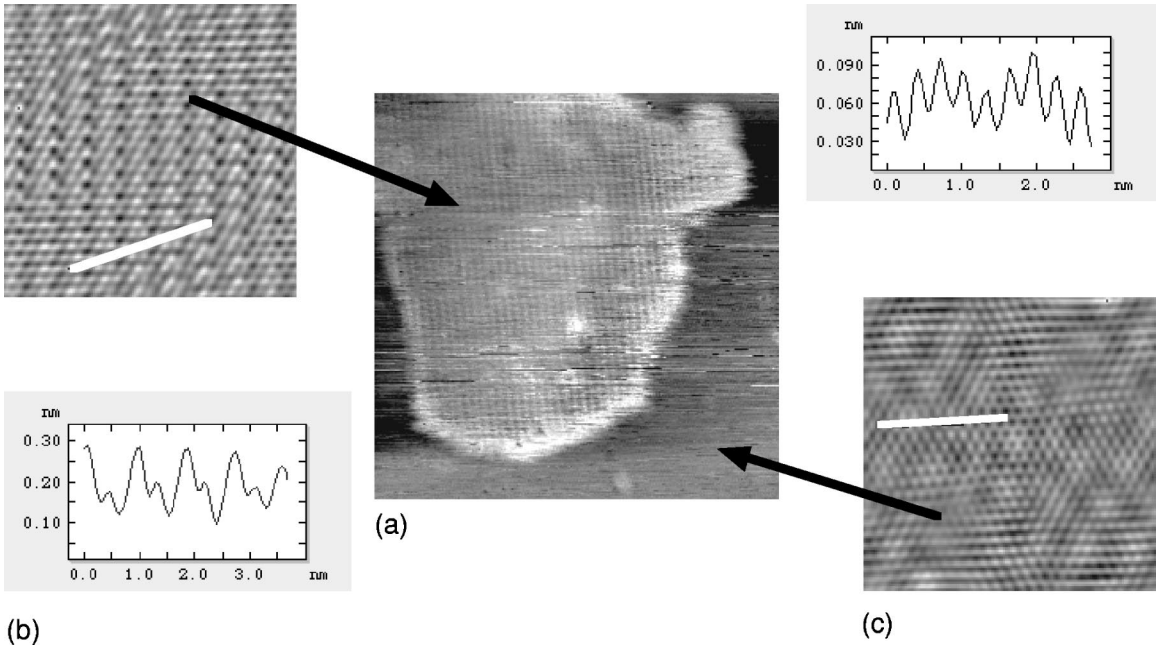

FIG. 5. Overview of the different CDW's in the two different areas. In the intercalated areas a strong octahedral CDW is found, while the nonintercalated areas exhibit a 4×4 CDW similar to the CDW in pure VSe_2. $80\,K<T<110\,K$. (a) Overview image, $46\times46\,nm^2$, $V_t=-366\,mV$, and $I_t=0.473\,nA$. (b) Na-induced CDW, $\sim7\times7\,nm^2$, $V_t=189\,mV$, and $I_t=0.789\,nA$. (c) Nonintercalated area CDW, $\sim7\times7\,nm^2$, $V_t=-161\,mV$, and $I_t=1.933\,nA$. White bars show the positions of the cross sections. Note that in (b) the cross section is shown along the direction of the CDW and not along any host lattice direction.

then be seen directly in the grayscale image together with the CDW in the intercalated parts (Fig. 10). At higher bias voltages the small corrugation in the NI areas could not be seen in the grayscale images, since it was ''hidden'' by the grayscale variation of the much stronger Na-induced CDW. The enhancement of the Na-induced CDW was obvious only when looking at line scans, but the relative enhancement was approximately the same in the two different types of areas, i.e., about five times.

Low-temperature STS (Fig. 4) showed different spectra in the NI and *I* areas. Below T_C, STS in the NI areas [Fig. 4 (curve *C*)] showed that the V $3d$ peak was slightly shifted toward E_F, to about -60 meV. Lowering the temperature further did not change the position of this peak. The CDW energy gap was never resolved in the NI parts of the material. Low-temperature STS at the *I* areas [Fig. 4 (curve B)] showed a large CDW energy gap, $\Delta\approx230$ meV. The V $3d$ peak was shifted also in the *I* areas, but here it was shifted

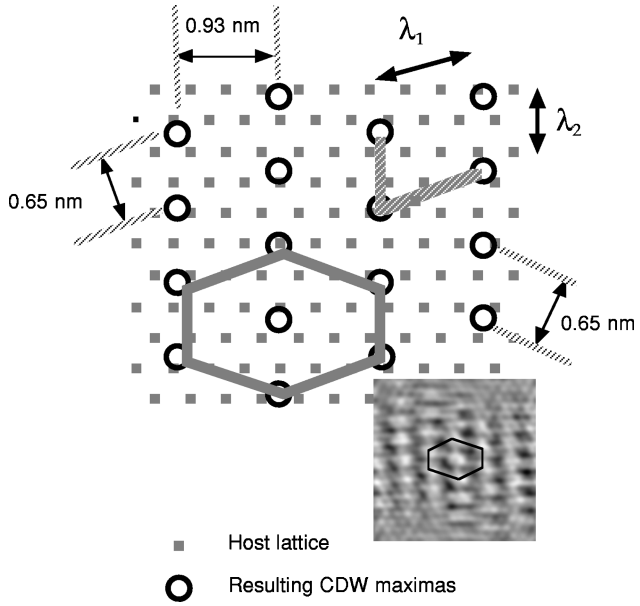

FIG. 6. The structure of the Na-induced CDW. The periodicities found in the FFT image are indicated by thin dashed lines. Where the three periodicities intersect, a CDW maxima will be found (circles). The resulting incommensurate structure is marked in the STM image and in the structure model. This structure can also be considered as an octahedral structure ($\lambda_1\approx0.99$ nm, $\lambda_2\approx0.68$ nm, $<70°$), rotated 20° counterclockwise with respect to the atomic lattice, marked with dashed lines in the structure model.

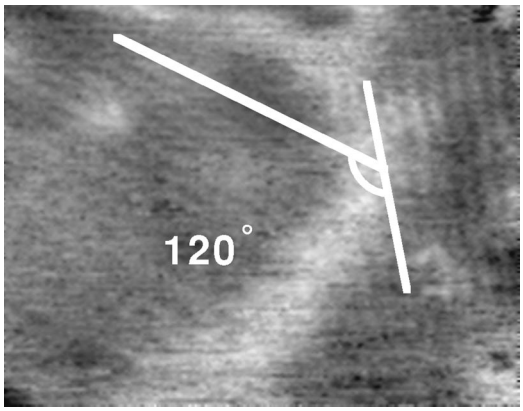

FIG. 7. Part of a Na island showing two domains of different CDW rotation, with an angle of 120° between the two directions. $V_t=-124\,mV$, $I_t=1.391\,nA$, scan size $\sim24\times18\,nm^2$ and $T=60\,K$.

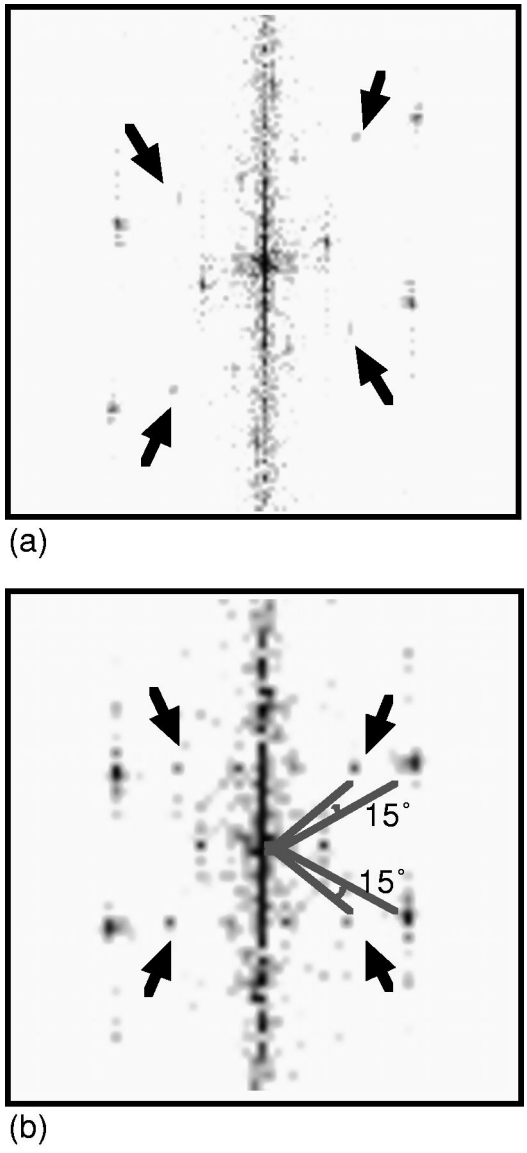

FIG. 8. FFT images taken from a Na island below T_C. (a) Unprocessed image (256×256 data points). (b) After distortion correction (128×128 data points, giving lower resolution). The outermost hexagon are the atomic spots, and the inner distorted hexagon contains the CDW spots. Apart from these spots, four distinct extra spots are found (marked by arrows) that correspond to a quadratic period of 0.44 nm. These spots are rotated +15° and −15°, respectively, with respect to two of the three host lattice symmetry directions, as marked in the figure.

away from E_F, to about −150 meV. Neither the gap nor the V 3*d* peak changed significantly with temperature.

IV. DISCUSSION

A. Room temperature

The room-temperature results were in line with our previous results, and were discussed in Ref. 24. In room-temperature images we can see streaks in the scanning direction. One might ascribe this to an effect of tip changes, so that the dark and bright areas are nothing else than changes in the tunneling junction, e.g., by jumping of Na or contaminants. The stability of the images (reproducible areas, atomic

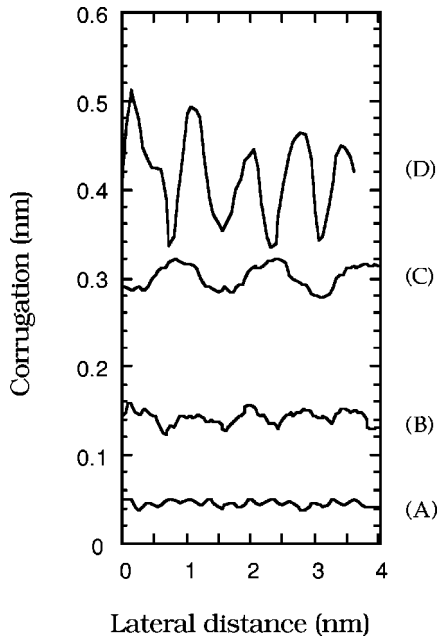

FIG. 9. Cross-section lines showing the corrugation for different scanning parameters. (*A*) Nonintercalated area at $V_t=-114$ mV and $I_t=1.341$ nA. (*B*) Intercalated area at $V_t=-189$ mV and $I_t=0.789$ nA. (*C*) Nonintercalated area at $V_t=-2$ mV and $I_t=2.786$ nA. (*D*) Intercalated area at $V_t=-2$ mV and $I_t=4.015$ nA. The CDW corrugation was greatly enhanced at lower bias voltages, i.e., at closer tip-sample distances.

resolution, and stable spectroscopy) together with the known diffusion constant of alkali atoms along TMD layers, 10^{-8} cm^2/s (Ref. 27), led us to the conclusion that the streaks are a result of mobile Na below the first layer, as discussed in an earlier paper.[25]

B. Low temperature

1. Charge-density waves and Na ordering

(a) *Local effects.* One of the more conspicuous conclusions from the low-temperature measurements is that the effect of Na intercalation seemed to be very local. While the

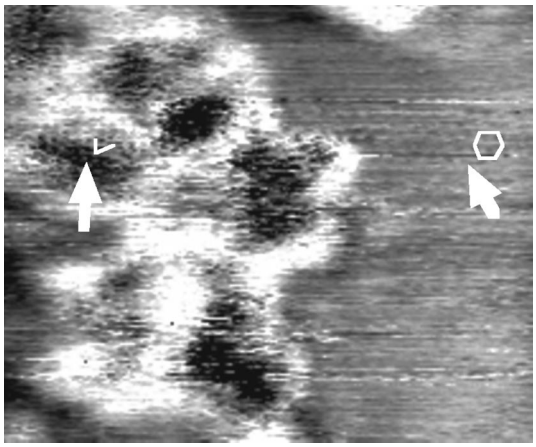

FIG. 10. STM image taken with $V_t=-2$ mV showing CDW modulations both at intercalated areas and at nonintercalated areas, marked by arrows. CDW structures are shown as a guide for the eye. The scan size is 45×55 nm^2.

Na intercalation induced a totally different CDW in the *I* islands, the NI parts seemed unaffected by the presence of Na in the material. The only sign of changes in the NI areas, compared to pure VSe_2, was the shifted V $3d$ peak. As far as our analysis can tell, the 4×4 CDW was the same as in the pure material, and we could not observe any obvious distortions of the CDW near the *I* islands. This indicates that local effects are dominating in the observed CDW. McMillan's short-coherence model for calculation of CDW properties at a finite temperature,[28] is usually considered to be valid for the TMD-CDW systems. This model gives correlation lengths of the order of the CDW unit-cell length, so that local effects would be expected, although the CDW formation is considered to be a long-range effect of electron-hole pairing. Local CDW effects upon intercalation was found by Koslowski *et al.*[29] using STM on Ag intercalation in $2H$-$NbSe_2$, showing islandlike structures with a different CDW than in the clean material. However, Koslowski *et al.* measured above the transition temperature of $2H$-$NbSe_2$, so the effect of intercalation in the NI areas are not investigated. Local effects were also shown by Zhang *et al.*[30] upon creation of nanocrystals of $1T$ coordination in $2H$-$TaSe_2$ by voltage pulsing with a STM tip, and the opposite transition, $1T\rightarrow2H$ were observed by Kim *et al.* in $1T$-TaS_2 (Ref. 31). These nanocrystals are well defined, and show sharp boundaries between the different phases. In very small crystals the CDW is distorted at the boundaries, and the corrugation amplitude also differs across the nanocrystal. A difference between those nanocrystals and the present situation is that we have Na atoms below the first layer. In our case the results can therefore not be solely an effect of coordination changes in one single TMD layer, as in the $TaSe_2$ and TaS_2 cases. That we did not find as sharp boundaries between our NI and *I* areas, as observed for the $TaSe_2$ and TaS_2 nanocrystals, is possibly associated with the fact that the Na atoms are situated *below* the first layer. We have to remember that the boundaries observed at the surface are not the authentic boundaries between Na atoms and the surroundings, but are an effect of the top layer buckling due to intercalation.

(b) *The structure of the induced CDW and the ordered Na superstructure.* Only a few STM studies of intercalation in TMD's have been reported. Intercalation of Ag in $1T$-TaS_2 lowers the different CDW transition temperatures compared to the pure material, and changes the Ta coordination from $1T$ to $2H$.[32] Bulk-intercalated Li in $1T$-TaS_2 induces a reduction of the CDW wavelength, from 11.5 to 10.3 Å at room temperature.[33] $2H$-TaS_2, that has a CDW transition at 75 K, intercalated by Ag shows an ordered 2×1 Ag structure but no CDW at room temperature.[34] Fe-intercalated $2H$ phases of $NbSe_2$, $TaSe_2$, and TaS_2 show a variety of superstructures at 300 and 4.2 K, originating from Fe ordering and CDW's.[35] Also Ag intercalation in NbS_2 has been studied, but this system does not exhibit a CDW.[36] Koslowski *et al.* studied stage-2 Ag intercalated $2H$-$NbSe_2$ (Ref. 29) at room temperature. This system shows a local CDW, different from the intrinsic 3×3 CDW that is found below 33 K, in areas where intercalated atoms are located below the surface. The CDW pattern in the Ag_xNbSe_2 system is a strongly disordered hexagonal pattern with an average wavelength $\lambda_{CDW}=1.25$ nm, a value close to that expected for a $\sqrt{13}\times\sqrt{13}$ superstructure. Atomic resolution together with the CDW is occasionally found, and the rotation with respect to the atomic lattice is $\sim15°$. This means that the CDW is similar to the one in the $1T$-Ta compounds, and the authors suggest that a stacking order and coordination change ($2H\rightarrow1T$) in the surface layers is responsible for the induced CDW. The disorder of the superstructure is expected to be connected to the order/disorder of the intercalated Ag. Pure $NbSe_2$ does not exist in the $1T$ phase, but upon intercalation the ''*T*-phase'' structure might be locally stabilized.

Our nonhexagonal and incommensurate Na-induced CDW structure is locally induced in a similar way to the CDW in the Ag_xNbSe_2 system. However, we do not believe our CDW to be a result of the same type of stacking order/coordination change, due to the lack of similarities to any other known TMD CDW's. In real space the CDW is an octahedral superlattice with $\lambda_1\approx0.99$ nm and $\lambda_2\approx0.68$ nm, $\angle70°$, rotated 20° counterclockwise with respect to the atomic lattice. Finding a CDW with a nontrigonal symmetry in a trigonally symmetric system might seem surprising, but this has been seen in different graphite intercalation compounds (GIC's). Lang *et al.*[37] found a number of different superstructures in bulk-intercalated alkali GIC's. Apart from a 2×2 superstructure, due to ordering known from diffraction studies, different hexagonal, orthorhombic, and one-dimensional superstructures are found, that are suggested to be surface-driven CDW's. Kelty and Lieber found an orthorhombic structure in $KHgC_4$, that occurs in two orientations with respect to the atomic lattice and also this is suggested to be a CDW.[38] A CDW of different symmetry than the atomic lattice is therefore a possibility, although it has previously not been observed among the TMD's. However, that we observe three different rotations of the CDW pattern is, we believe, due to the trigonal symmetry of the atomic host lattice. The white protrusions in Fig. 7 separate different *I* domains, and are less than 0.5 Å high. This apparent increase in height might be due to a different Na concentration or coordination at the domain boundaries, but may also be a purely electronic effect. At the boundaries between NI and *I* areas no such protrusions are found.

The extra spots in the FFT are explained as an effect of Na ordering. Three facts support this idea. First, the extra spots were only visible in the *I* areas, and, second, the rotation of the spots with respect to the atomic lattice followed the rotation of the Na-induced CDW with respect to the atomic lattice. Both these observations suggests that an ordered Na superlattice was the origin of the spots. Third, they only appeared at low temperatures, and at the same time streaks in the scanning direction are less pronounced. These spots could not originate from the sum of other FFT spots, neither were they a sum of other spots and a lattice vector. This periodicity was only found in the FFT and not in real space. By inverse transformation of images, where only the spots corresponding to the host atoms and the ''Na'' were selected, we attempted to avoid the strong CDW to hide a possible superstructure in real space. However, no visible superstructure was observed. Dai *et al.* observed a 2×2 superlattice due to ordering in Fe-intercalated samples of the $2H$-phases of $NbSe_2$, TaS_2, and $TaSe_2$ by STM and atomic force microscopy (AFM).[35] In $TaSe_2$ the amplitude of the superlattice was barely detectable at room temperature, while low-temperature STM scans, as well as room-temperature

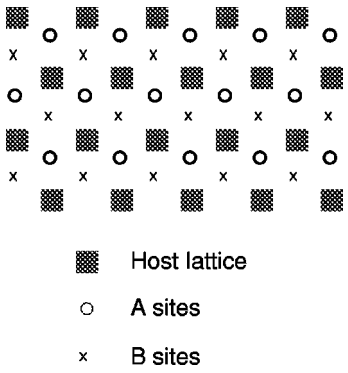

FIG. 11. Possible sites for Na between the host layers in VSe_2. For low coverages, both *A* and *B* sites can be occupied, but not neighboring sites due to the short Na-Na distance.

AFM scans, showed larger modulations. This was interpreted as a large static transfer of charge to the surface Se atoms, observed by AFM, while the local density of states modification at E_F, responsible for STM response, was small at room temperature and increased at low temperatures for $TaSe_2$. We cannot exclude the possibility of this being the origin also for our low-temperature observation of ordering. Although no observation supports it, the Na could be ordered even at room temperature, but in any case Na ordering would be the origin of the observation of extra FFT spots at low temperature.

Intercalated Na_xVSe_2 is expected to exhibit one of the trigonal prismatic $3R$(I) or octahedral $3R$(II) structures.[21] In our case, we believe that we have the $3R$(I) structure for two reasons. First, this structure is usually found in intercalation compounds with low alkali-metal concentration. Second, the expansion along the *c* axis, caused by the Na atoms being too large to fit in the van der Waals gap, is different in the two structures, and the *c*-axis lattice parameter of the $3R$(I) structure fits best to our measurements, as has been reported earlier.[24] It has been suggested that the $3R$(I) phase of Na_xVSe_2 exhibits CDW's,[20,22,23] but any structure of such a CDW has not been reported. In the $3R$(I) structure the intercalated Na atoms occupy trigonal prismatic sites between the host atomic layers. In stoichiometric $NaMX_2$ either *A* or *B* sites (Fig. 11) will be occupied. For $x<1$ both *A* and *B* sites can be occupied, but not neighboring sites, since the distance between the alkali atoms would then be too small. Diffusion of Na along the layers is then likely to proceed by jumps of type $A \leftrightarrow B$.[21] According to Bloembergen, Haange, and Wiegers,[21] Na in TMD's will be ordered in a $2\times\sqrt{3}$ structure. Hibma[39] showed that in Na_xTiS_2 for $x<0.25$, Na ordering in 2×2 and $\sqrt{3}\times\sqrt{3}$ superstructures is found, while for $0.25<x<0.5$ a $2\times\sqrt{3}$ structure, in different rotations, is found. Since we are evaporating ~1 ML, we probably have Na only in the *surface layers*, and the density of Na is fairly low. According to our earlier PES measurements,[24] $x \approx 0.25$. This cannot be directly compared to the STM measurements for two reasons. First, in the PES measurements we are comparing the Na $2p$ and Se $3d$ core-level signals, and since the penetration depth is small in PES, more Se will be detected in the photoemission spectra. Two Se layers exist close to the surface before Na appears in the first van der Waals gap, and also the next Se layer, below the first van der Waals gap, contributes in PES. Second, the PES signals are averaged over the entire surface, i.e., the two different areas are mixed. Therefore, it is likely that we have a higher concentration in the *I* areas than PES indicates. We believe the Na concentration to be $x\approx0.5$ in the topmost layer of the *I* islands. The ordered structures, according to Hibma and Bloembergen, therefore will not be directly applicable in our case. According to Wiegers,[20] the $3R$(I) structure is found for $0.5\leqslant x\leqslant0.6$, and the $3R$(II) structure for stoichiometric ($x=1$) Na_xVSe_2. Mixtures of VSe_2 and $3R$(I) (low concentrations) and $3R$(I) and $3R$(II) (high concentrations) are found in between. We note that what we observe is actually the mixture of pure VSe_2 and the $3R$(I) structure.

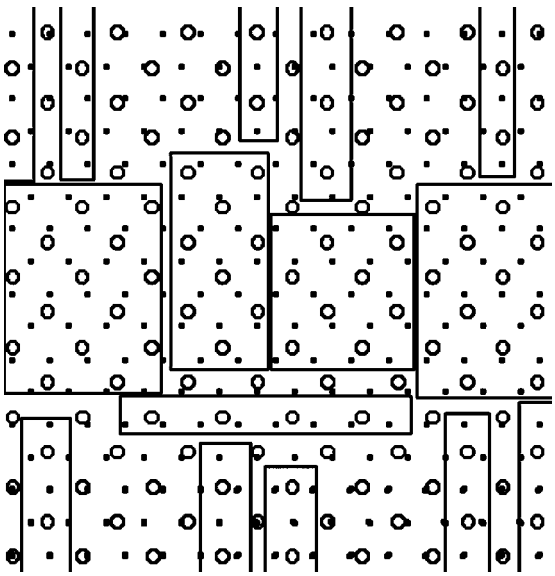

FIG. 12. Combination of the host lattice (dots) and the 1.3×1.3 $R45°$ Na structure (circles). Rectangles enclose the allowed Na positions, i.e., when the superstructure does not coincide with the host lattice. The resulting structure is essentially domains of alternating *A* and *B* positions, but with positions slight off-center allowed.

Our FFT observations could be translated into a 1.3×1.3 $R45°$ structure in real space. To test whether this structure was possible, we draw the atomic lattice together with this structure. When the atomic lattice and the ''Na position'' coincided, the ''Na atom'' was not allowed to sit there, while a position slightly off center in the octahedral holes was allowed, although pure *A* or *B* sites presumably are preferred. As the ''Na-Na distance'' is slightly larger than the lattice parameter, Na is allowed to sit in a 1.3×1.3 $R45°$ structure with no coincidence with the host lattice for about seven unit cells, i.e., 2–3 nm. After this distance the Na will sit in a forbidden position, and the periodicity will be broken. However, leaving one row empty in the host lattice before the next Na atom is inserted will restore the periodicity. The structure then consists of small domains with alternating rows of *A* and *B* coordination (Fig. 12). At the interfaces of these small Na domains, rotations of the structure can be allowed, as observed in the STM images. This domain structure could also explain the appearance of islands, as well as the appearance of holes of locally missing Na in between different domains. However, the holes might also be an effect of excess V in the van der Waals gap, since VSe_2 grows metal rich. To our knowledge, no other structures than the

ones discussed ($2\times\sqrt{3}$,2×2,$\sqrt{3}\times\sqrt{3}$) have been reported. Still, our structure explains the observed data, and the low Na concentration might give possible ordered structures. Our 1.3×1.3 $R45°$ structure is therefore the most plausible explanation, and we can note that neither the $2\times\sqrt{3}$ nor our 1.3×1.3 $R45°$ structure is hexagonal, as one might expect from the symmetry of the host lattice. The periodic lattice distortion that is accompanying the CDW changes the lattice, and might allow the Na atoms to occupy positions slightly off center from the pure *A* and *B* sites more easily. This lattice distortion is too small to be resolved with STM, especially when considering our image distortion. One could argue that a third pair of spots, giving a distorted hexagonal pattern for the ''Na ordering,'' could be hidden along the vertical line in the FFT image (Fig. 8). However, these spots would then be visible in the 120° rotated pattern, which is not the case. The only possibility of a third pair of spots in the rotated image would be if they coincided with the atomic spots. Using that periodicity gives a real-space structure that is even harder to fit in the host lattice than the square structure. Also, the 90° difference of the ''Na spots'' in the FFT suggests that a square symmetry would be most plausible.

Due to the $3R$(I) structure, Na_xVSe_2 cannot be directly compared with the other types of ordinary TMD-CDW materials. The induced CDW showed some similarities to the $1T$-Ta compounds, i.e., rotation, strong corrugation, and a large energy gap. The nonhexagonal structure can, however, not be explained by comparisons to other TMD-CDW systems, as discussed above. One can note that $1T$-VSe_2 itself is a very special material, e.g., in many ways it behaves more like the $2H$ compounds than the $1T$-Ta compounds. VSe_2 occurs only in the $1T$ phase, but has an exceptional value of c/a (1.82 compared to 1.75 for $1T$-TaS_2, 1.80 for $1T$-$TaSe_2$, 1.633 for the ideal $1T$ structure, and 1.82–1.85 for the $2H$ structure), and shows a low T_C, small corrugation of the CDW, no rotation with respect to the atomic lattice, and a small energy gap. All those properties are more similar to the $2H$-phase materials than the $1T$ materials.

(c) *T_C and IC-C transitions.* Finding an exact T_C is difficult by using STM and STS, since the actual tip conditions are crucial, and image quality can change during scanning in an unpredictable way. However, the observed T_C seems to be roughly the same in the NI and *I* parts of Na_xVSe_2, and also the same as in pure VSe_2, i.e., ~110 K. It might be surprising that T_C was the same in the *I* and NI areas, especially when considering the large energy gap in the *I* areas, that usually goes with a higher T_C. Wiegers[20] found anomalies in the magnetic susceptibility vs *T* for Na_xVSe_2, ascribed to a CDW. The temperature anomaly depends on *x* in a nonlinear fashion. This is probably connected to the different structures of Na_xVSe_2 at various concentrations, and it is therefore hard to conclude whether our observed T_C agrees with the expectations.

No IC-*C* transitions could be observed either in the pure VSe_2 or in the NI areas of Na_xVSe_2. Due to the drift in the microscope it is very difficult to measure the exact CDW wavelengths with enough accuracy, so this is probably better done with other surface-sensitive techniques, e.g., diffraction techniques. However, most other techniques suffer from a lack of site-specific measurements, and the NI and *I* areas would be studied simultaneously. We believe that any transition would be common for the pure VSe_2 and the NI parts of Na_xVSe_2, due to the similarities of the CDW. The Na-induced CDW is completely incommensurate in the temperature range investigated. It would of course be interesting to look for possible IC-*C* transitions in the *I* parts at lower temperatures. The 60-K limit of our experiment ensures that we are well below the possible IC-*C* transition at 80 K in the pure sample. The lower limit of our STM is around 30 K, but below 60 K we found it more difficult to obtain stable temperatures. Therefore we cannot exclude further transitions occurring at a lower temperature, but there are also examples of CDW's that are incommensurate down to the mK range, e.g., the $2H$ phases of TaS_2 and $NbSe_2$.[9]

2. Corrugation enhancement

Materials such as graphite, $1T$-$TaSe_2$, and $1T$-TaS_2 can show anomalous corrugations that are too large to be characteristic of the surface atomic structure.[40,41] Tersoff[42] suggested that this is due to an electronic effect in materials where the Fermi surface collapses to a point at the corner of the surface Brillouin zone (BZ), which is possible for a semiconductor or semimetal of reduced dimensionality. The STM image in this case will correspond to a single wave function, having nodes leading to large corrugations across the unit cell defined by the Fermi surface. In a quasi-two-dimensional material, such as the TMD's, the wave functions can be expanded into six plane waves, and, if the band edge falls near the BZ corners the model will generate a hexagonal array of singular dips.[41] This means that the Fermi-surface collapse will not be complete, but the nodal structure will depend on the degree of Fermi-surface elimination. This effect should however be independent of the tip-sample distance. Soler *et al.*[43] suggested corrugation enhancement by a mechanical, elastic, tip-sample contact at low bias making the actual tunnel distance variations smaller than the response of the piezo. The contact area is assumed to be on the atomic scale. Pethica[44] argued that the actual tip-sample contact area would be large, and that the main reason for the corrugation enhancement would then be an effect of shear in the stacking layers. A flake of the layered material transferred to the tip would give the expected periodicity while imaging, since what is detected is the fluctuation in conductance between tip and sample. We reject this explanation, since we observe defects, that would not be expected if a flake of the material were located at the tip. Mamin *et al.*[45] explained corrugation enhancement by tip-sample contact mediated by contamination. According to their model, tunneling occurs from a protruding miniature tip, through a contamination layer that causes tip-sample contact. Their measurements after cleaning the tip and the graphite surface in vacuum showed a much lower corrugation than in air for the same tunneling conditions, leading to the conclusion that significant distortion of the surface by mechanical tip-sample contact is present only when there is a contamination layer. We cleave our samples in air, and, even if the sample is heated, there might still be some contamination at the surface, so that this mechanism could be possible. However, all the mechanisms of tip-sample contact are also likely to affect the atomic corrugation, which is not observed in our measurements. Apart from the contamination mechanism, the contact mechanisms assume a poor conductor. VSe_2 is metallic below the transition

TABLE I. Summary of our STS and some earlier experimental and theoretical results.

	$V\,3d$ state, RT(meV)	$V\,3d$ state, 60 K(meV)	Energy gap Δ (meV)	$2\Delta/k_BT_C$	Ref
Pure VSe_2	−85	−80	80 (60 K)	17	
Pure VSe_2			40 (4.2 K)	8.4	8
Clean areas of Na_xVSe_2	−80	−60			
Na area of Na_xVSe_2	−90	−150	230 (60 K)	48	
Pure VSe_2, theory	−170				14
$NaVSe_2$, theory	−380				14
$2H$-$TaSe_2$, theory				30	25

temperature, stoichiometric $NaVSe_2$ is considered as a semiconductor, and Na_xVSe_2 for $0.5 \leqslant x < 0.6$ is metallic.[22] The mixed phases for $x < 0.5$ are therefore expected to be metallic, since both VSe_2 and the $3R$(I) structure are metallic, while the higher concentration mixed phases are possibly semiconducting. We have a low concentration sample and expect the entire sample to be metallic. Tip-sample contact mechanisms can therefore not be the *main* cause for our observation of corrugation enhancement, but an electronic effect is needed to explain the results. Still, despite that the approach of Tersoff can explain the large corrugations observed in the $1T$-Ta compounds and graphite, the approach with mechanical contact is needed to explain the distance dependence, that is well established at least for graphite.[40] Therefore, a combination of contact and electronic effects might be the solution of the corrugation enhancement.

Giambattista *et al.* measured a rapid change of tunneling barrier with distance in VSe_2.[41] The tunneling barriers for the $1T$-Ta compounds are found to have much slower variation, and the conclusion is that the presence of a strong CDW causes this slower variation, and thereby a lower response to tip-sample distance variations.[41] The width of the energy gap in our *I* areas is of the same order as for the Ta compounds, despite the metallic character, and we have a fairly strong CDW in these areas. We might therefore expect more similarities to the $1T$-Ta compounds in the *I* areas. However, we found a percentage corrugation enhancement of ~500% at low bias in both *I* and NI areas. A measurement of the tunneling barrier vs distance in the different areas of our Na_xVSe_2 sample could give a clue to the expected behavior of the *I* islands compared to the NI parts. Obviously, the corrugation enhancement in the CDW systems are a complex matter that needs further study. The corrugation enhancement is not crucial for the conclusion of the structure and behavior of the CDW's, but is an observation that might give additional clues to the understanding of STM response to CDW's and also of the CDW's themselves.

3. Energy gaps and the V 3d state

In all STS measurements the structures in the tunneling spectra were rather broad. We chose values for the structures in the middle of the peaks for the V $3d$-derived state, and in the middle of the flat range in the spectra for the energy gaps. Our STS measurements are summarized together with some other experimental and theoretical results in Table I. To account for measurement uncertainties, we made statistics of the measured values, and what is given here is the median values, cf. Fig. 13. Wang, Slough, and Coleman studied pure VSe_2 by STS.[10] They reported an energy gap $\Delta = 40$ meV at 4.2 K that does not agree with our measured gap, $\Delta \approx 80$ meV. CDW gaps have a BCS-like temperature dependence, i.e., increasing gaps when decreasing the temperature, so our gap would then be expected to be smaller than 40 meV. The measurement of Ref. 10 was done with a voltage range of less than ±100 meV and did not resolve the V $3d$ state. That we see the V $3d$ peak ensures us that at least a part of the band structure is reflected in the data, but at the same time this peak complicates the estimate of the gap. We have tried smaller voltage ranges to see if we could find a smaller gap inside the structure we ascribe to the gap, but all

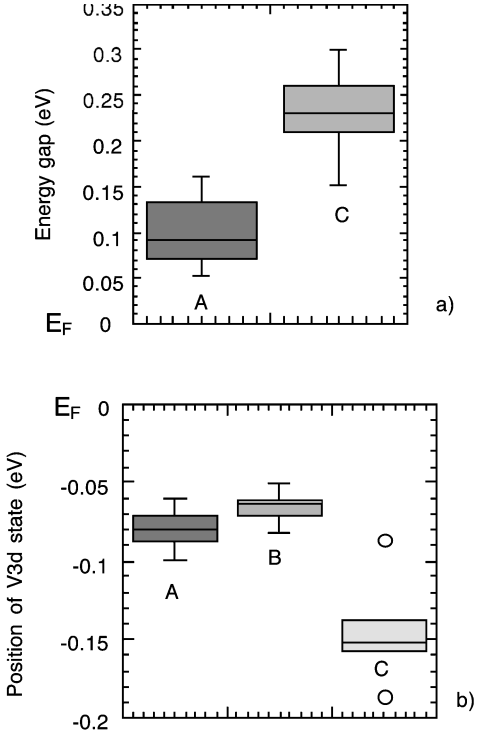

FIG. 13. Statistics from spectroscopy measurements that clearly shows the trends of the shifts. (a) Energy gaps in pure (*A*) and intercalated (*C*) samples. (Nonexisting gap in NI areas not shown.) (b) Position of the V $3d$ state in the different samples. (*A*) Pure VSe_2. (*B*) NI areas of Na_xVSe_2. (C) *I* areas of Na_xVSe_2. The box encloses 50% of the values, horizontal lines correspond to median values, and vertical lines extending from the box mark the maximum and minimum values. single values far away from the rest are marked as circles [occurs in curve *C* in (b)].

we could see was the tail of the V $3d$ state. We find it puzzling that the V $3d$ state is not resolved in the spectra of Ref. 10, but prominent in our spectra. The presence of the peak could give an overestimate of the gap, since we mostly base the gap on the structure seen above E_F. However, the gap should be symmetrical, and can not be much smaller than the estimated $\Delta \approx 80$ meV. Also, the spectra are reproducible with different tips and samples. To our knowledge, the spectra of Ref. 10 is the only published energy gap for VSe_2. However, one should note that the interpretation of STS spectra is far from trivial, and measurements of energy gaps in high-T_C superconductors have given values that differ considerably.[46]

The unsuccessful attempts to resolve the energy gap in the NI areas of Na_xVSe_2 does not necessarily have to be an effect of an intercalation-induced change of the gap. The low-temperature measurements of the pure VSe_2 sample showed that resolving the gap is highly dependent on the tip. Thus the lack of a gap could be an effect of not having the appropriate tip for resolving the gap in the NI parts. However, it could also be an effect of the shifted V $3d$ state approaching E_F, making the gap difficult to resolve. A CDW gap need not necessarily be much more than a weak depletion at E_F, and the reason that we expect an gap is the observation of the 4×4 CDW modulation in the topographic images. Considering the similarities of this CDW and the pure CDW, we expect the electronic structures to be roughly the same.

The Na_xVSe_2 gap was found to be large, $\Delta \approx 230$ meV, compared to the $\Delta \approx 80$ meV gap for pure VSe_2. This gap is of the same order as the gaps in the $1T$-Ta compounds, that have been measured to $\sim$150–200 meV in $1T$-TaS_2 and $1T$-$TaSe_2$ (Refs. 47 and 48). However, this large energy gap also suggests a higher T_C than observed here. Our energy gap and T_C gives a value of $2\Delta/k_BT_C = 48$, which is extremely high. The value of $2\Delta/k_BT_C$ for the $1T$-Ta compounds are $\sim$6, according to Ref. 10, while pure VSe_2 has $2\Delta/k_BT_C \approx 17$, according to our measurements, a value close to the $2H$ compounds that have $2\Delta/k_BT_C \approx 15$–$25$ (Ref. 10). Miyahara, Bando, and Ozaki[49] measured a value of $2\Delta/k_BT_C = 57$ in the semiconducting $1T$-$TiSe_2$ using a planar tunneling junction. The energy gap of Ref. 49, however, is largely dependent on temperature, and approaches a value of $\sim$25 at T_C, more consistent with optical measurements of the same material. Our sample is evidently different from ordinary TMD's, and the surroundings of the I islands could give effects keeping T_C at a lower temperature although the gap is increased. According to the theory by McMillan,[28] $2\Delta/k_BT_C \approx 30$, which is in between our value and the ones observed for the pure TMD's. The gap edge was quite broad in our measurements, so by choosing another criterion for the gap edge than in the middle of the flat range, e.g., choosing the value closest possible to the point where depletion starts, the energy gap can become significantly smaller, down to as low values as $2\Delta/k_BT_C \approx 30$. This is still a large gap, but in excellent agreement with the theory of McMillan. The VSe_2 transition is a metal-metal transition, although most TMD's become semimetallic after the CDW transition, and we still have a fairly high density of states at E_F below T_C after intercalation, indicating that Na_xVSe_2 also has a metal-metal transition.

The state below E_F originates from a mainly V $3d$-derived band. Near the Brillouin-zone center, the electrons have a parallel wave-vector component $k_\parallel \approx 0$. These electrons tunnel much more effectively than electrons with large $k_\parallel$, and dominate the STM imaging and spectroscopy. Henceforth, when we discuss the calculated energy of the V $3d$ state, we refer to the energy at the center of the Brillouin zone, i.e., at the Γ point. The V $3d$ state is found about 100 meV below E_F from various theoretical and experimental studies.[12,13,17–19] Calculations[17] of the undistorted VSe_2 and stoichiometric $NaVSe_2$ predict a shift of the V $3d$ state from -170 meV in pure VSe_2 to -380 meV in $NaVSe_2$ as a consequence of intercalation (cf. Table I). This is not the case in our observations. The small variations in the position of the V $3d$ state at room temperature cannot be considered significant. Instead, a shift of the V $3d$ state, from -90 to -150 meV in the I areas, is found below the CDW transition temperature. We have no ready explanation why we only find this shift below T_C. The V $3d$ state is located within the energy gap (i.e., inside the density of states depletion) in the I areas, and is therefore likely to be influenced by the CDW formation, as in our observation. Still the calculations predict the shift as a consequence of intercalation itself, and not of the CDW formation. In the NI areas the shift is small, from -80 to -60 meV, and one could argue that it is just a measurement artifact. The statistics from different tips and samples (Fig. 13) convince us, however, that the shift exists, since the state clearly appeared at lower energies than in the pure samples. In our earlier paper[25] we suggested a shift of -60 meV also to be present at room temperature. With larger statistics this shift at room temperature is not clear. The differences in the absolute positions of the V $3d$ state in the calculations and experiments are not very surprising. First, the calculations consider a stoichiometric sample, and, as electrons are transferred to the host lattice upon intercalation, the V $3d$ state must have a higher binding energy in a stoichiometric sample than in a nonstoichiometric sample, i.e., the state will be shifted further away from E_F in a stoichiometric sample. Second, the calculations assume a $1T$ crystal structure, while we are most likely to have a $3R$(I) structure as discussed above. We note that the PES data for the V $3d$ band is in lesser agreement with the calculations than for the Se $4p$-derived valence bands at higher binding energies, and that no shift of the V $3d$ peak has been resolved in the PES measurements done at room temperature.[17] The PES determined V $3d$ band is very narrow, which also favors the short-coherence model of McMillan.[28] Still, we have no explanation of why there is a shift away from E_F in the I areas, and toward E_F in the NI areas. We have observed that the ordering of Na atoms at low temperatures induces a charge ordering, but it appears that it also involves a mechanism where charge is transferred from the NI areas to the I areas. Unfortunately there are, to our knowledge, no theoretical or experimental studies available, either for pure VSe_2 or the intercalated material, probing the low-temperature effects on the band structure. The expected effects at low temperatures are therefore not known. We would also like to stress that STM has a unique possibility to distinguish between the different areas, which is not possible for most other experimental techniques, so that it would be difficult to compare any other results directly with STM measurements.

V. CONCLUSIONS

We have demonstrated a local modification of the CDW in Na-intercalated VSe_2 together with a nonhexagonal ordering of Na below the first layer at low temperatures. While the NI parts of the sample seemed unaffected by the presence of Na in the material, the *I* areas showed a strong, octahedral, CDW, rotated with respect to the atomic lattice. STS showed local effects on the band structure, with a different shift of the V $3d$-derived state below E_F in the different areas. A large energy gap was found in the *I* areas, in agreement with the short-coherence model of McMillan, while no gap was ever resolved in the NI parts. Corrugation enhancements of the CDW at low bias were found in both *I* and NI areas. This was not believed to be of pure tip-sample contact origin, but also due to electronic effects. The results clearly showed the local properties of both the intercalation-induced CDW and the undistorted CDW in the NI areas.

ACKNOWLEDGMENTS

We thank Dr. H. Starnberg for providing the VSe_2 crystals. I.E. acknowledges financial support from the Swedish Foundation for Strategic Research (SSF) Microelectronics program.

*Electronic address: ekvall@fy.chalmers.se

[1] C. Pettenkofer, W. Jaegermann, A. Schellenberger, E. Holub-Krappe, C. A. Papageorgopoulus, M. Kamaratos, and A. Papageorgopoulus, Solid State Commun. **84**, 921 (1992).
[2] H. I. Starnberg, H. E. Brauer, L. J. Holleboom, and H. P. Hughes, Phys. Rev. Lett. **70**, 3111 (1993).
[3] D. J. Eaglesham, R. L. Withers, and D. M. Bird, J. Phys. C **19**, 359 (1986).
[4] J. van Landuyt, G. A. Wiegers, and S. Amelinckx, Phys. Status Solidi A **46**, 479 (1978).
[5] K. Tsutsumi, Phys. Rev. B **26**, 5756 (1982).
[6] P. M. Williams, in *Crystallography and Crystal Chemistry of Materials with Layered Structure*, edited by F. Levy (Reidel, Dordrecht, 1976).
[7] A. H. Thompson and B. G. Silbernagel, Phys. Rev. B **19**, 3420 (1979).
[8] R. H. Friend, D. Jerome, D. M. Schleich, and P. Moline, Solid State Commun. **27**, 169 (1978).
[9] R. V. Coleman, Z. Dai, W. W. McNairy, C. G. Slough, and C. Wang, in *Scanning Tunneling Microscopy*, edited by J. A. Stroscio and W. J. Kaiser (Academic, San Diego, 1993).
[10] C. Wang, C. G. Slough, and R. V. Coleman, J. Vac. Sci. Technol. B **9**, 1048 (1991).
[11] J.-J. Kim, C. Park, and H. Olin, J. Korean Phys. Soc. **31**, 713 (1997).
[12] H. P. Hughes, C. Webb, and P. M. Williams, J. Phys. C **13**, 1125 (1980).
[13] M. T. Johnson, H. I. Starnberg, and H. P. Hughes, J. Phys. C **19**, L451 (1986).
[14] R. Claessen, I. Schäfer, and M. Skibowski, J. Phys.: Condens. Matter **2**, 10 045 (1990).
[15] A. R. Law, P. T. Andrews, and H. P. Hughes, J. Phys.: Condens. Matter **3**, 813 (1991).
[16] H. I. Starnberg, P. O. Nilsson, and H. P. Hughes, J. Phys.: Condens. Matter **4**, 4075 (1992).
[17] H. E. Brauer, H. I. Starnberg, L. J. Holleboom, V. N. Strocov, and H. P. Hughes, Phys. Rev. B **58**, 10 031 (1998).
[18] A. M. Woolley and G. Wexler, J. Phys. C **10**, 2601 (1977).
[19] A. Zunger and A. J. Freeman, Phys. Rev. B **19**, 6001 (1979).
[20] G. A. Wiegers, Physica B & C **99**, 151 (1980).
[21] J. R. Bloembergen, R. J. Haange, and G. A. Wiegers, Mater. Res. Bull. **12**, 1103 (1977).
[22] C. F. van Bruggen, J. R. Bloembergen, A. J. A. Bos-Alberink, and G. A. Wiegers, J. Less-Common Met. **60**, 259 (1978).
[23] C. F. van Bruggen, C. Haas, and G. A. Wiegers, J. Solid State Chem. **27**, 9 (1979).
[24] H. E. Brauer, I. Ekvall, H. Olin, H. I. Starnberg, E. Wahlström, H. P. Hughes, and V. N. Strocov, Phys. Rev. B **55**, 10 022 (1997).
[25] I. Ekvall, H. E. Brauer, H. Olin, H. I. Starnberg, and E. Wahlström, Appl. Phys. A: Solids Surf. **66**, S197 (1998).
[26] I. Ekvall, E. Wahlström, D. Claesson, H. Olin, and E. Olsson, Meas. Sci. Technol. **10**, 11 (1999).
[27] R. H. Friend and A. D. Yoffe, Adv. Phys. **36**, 1 (1987).
[28] W. L. McMillan, Phys. Rev. B **16**, 643 (1977).
[29] B. Koslowski, W. Xu, B. Blackford, and M. H. Jericho, Phys. Rev. B **54**, 11 706 (1996).
[30] J. Zhang, J. Liu, J. L. Huang, P. Kim, and C. M. Lieber, Science **274**, 757 (1996).
[31] J.-J. Kim, C. Park, W. Yamaguchi, O. Shiino, K. Kitazawa, and T. Hasegawa, Phys. Rev. B **56**, R15 573 (1997).
[32] M. Remskar, V. Marinkovic, A. Prodan, and Z. Skraba, Surf. Sci. **324**, L367 (1995).
[33] X. L. Wu and C. M. Lieber, J. Am. Chem. Soc. **110**, 5200 (1988).
[34] W. Han, E. R. Hunt, S. E. Ulloa, and R. F. Frindt, Phys. Rev. B **45**, 14 415 (1992).
[35] Z. Dai, Q. Xue, Y. Gong, C. G. Slough, and R. V. Coleman, Phys. Rev. B **48**, 14 543 (1993).
[36] M. Remskar, V. Marinkovic, and A. Prodan, Surf. Sci. **352-354**, 1012 (1996).
[37] H. P. Lang, R. Wiesendanger, V. Thommengeiser, and H. J. Güntherodt, Phys. Rev. B **45**, 1829 (1992).
[38] S. P. Kelty and C. M. Lieber, J. Vac. Sci. Technol. B **9**, 1068 (1991).
[39] T. Hibma, J. Solid State Chem. **34**, 97 (1980).
[40] G. Binnig, H. Fuchs, C. Gerber, H. Rohrer, E. Stoll, and E. Tosatti, Europhys. Lett. **1**, 31 (1986).
[41] B. Giambattista, C. G. Slough, W. W. McNairy, and R. V. Coleman, Phys. Rev. B **41**, 10 082 (1990).
[42] J. Tersoff, Phys. Rev. Lett. **57**, 440 (1986).
[43] J. M. Soler, A. M. Baro, N. Garcia, and H. Rohrer, Phys. Rev. Lett. **57**, 444 (1986).
[44] J. B. Pethica, Phys. Rev. Lett. **57**, 3235 (1986).
[45] H. J. Mamin, D. W. Abraham, J. Clarke, E. Ganz, and R. E. Thomson, Phys. Rev. B **34**, 9015 (1986).
[46] P. J. M. van Bentum and H. van Kempen, *Scanning Tunneling Microscopy I*, 2nd ed. (Springer-Verlag, New York, 1994), Vol. 242, p. 207.
[47] C. Wang, B. Giambattista, C. G. Slough, and R. V. Coleman, Phys. Rev. B **42**, 8890 (1990).
[48] J.-J. Kim, I. Ekvall, and H. Olin, Phys. Rev. B **54**, 2244 (1996).
[49] Y. Miyahara, H. Bando, and H. Ozaki, J. Phys.: Condens. Matter **7**, 2553 (1995).